



Contents lists available at ScienceDirect

# International Journal of Rock Mechanics & Mining Sciences

journal homepage: [www.elsevier.com/locate/ijrmms](http://www.elsevier.com/locate/ijrmms)

## Space–time clustering of seismic events and hazard assessment in the Zabrze-Bielszowice coal mine, Poland

Andrzej Leśniak<sup>a,b,\*</sup>, Zbigniew Isakow<sup>b</sup><sup>a</sup> AGH University of Science and Technology, al. Mickiewicza 30, 30-059 Kraków, Poland<sup>b</sup> EMAG Centre, ul. Leopolda 31, 40-189 Katowice, Poland

## ARTICLE INFO

## Article history:

Received 29 March 2008

Received in revised form

13 December 2008

Accepted 23 December 2008

## Keywords:

Source location

Clustering

Seismic hazard

Rockbursts

Coal mining

## ABSTRACT

The results of the statistical analysis of seismic activity recorded in the “Zabrze-Bielszowice” coal mine in Poland are presented in this article. The monitoring was conducted by a small network consisting of four triaxial geophones deployed in vertical holes in the roof. For over 1000 seismic events recorded during the two month’s experiment, the location of sources was realized. The seismic sources were mostly located ahead of the active face of the longwall. Since the first day of the monitoring, cluster analysis was sequentially performed for increasing number of sources. At the end of the experiment, 31 clusters were identified. They consisted of different numbers of events and were separated in space. About 40% of the events were not included in the clusters. For each large cluster, hazard analysis was separately performed. The hazard function evaluated for the largest cluster was compared with hypocenters of high energy tremors ( $E > 1000\text{J}$ ) recorded by the geophones in that area. For some cases, recorded tremors occurred after an abrupt decrease of hazard function, but only one of them was located in the vicinity of the appropriate cluster. We concluded that for the analyzed cluster, a correlation between evaluated hazard function and time occurrences of the high energy tremors existed. Except for one case, there is no space correlation between analyzed clusters and high energy tremors.

© 2008 Elsevier Ltd. All rights reserved.

### 1. Introduction

For many years, worldwide community interested in mining safety research has attempted to develop technology that would provide warnings about impending tremors, rockbursts, coal bumps and gas outbursts [1]. Many different methods and techniques have been tried with different degrees of success [1]. A significant obstacle to applying tremors and other phenomena warning techniques is the lack of detailed knowledge concerning the stress distribution in the rock mass, their mechanical properties and structure. Progressing underground excavation is the direct reason of the lack of equilibrium of stresses in the vicinity of the wall. For the long wall excavating system, the most intense accumulation of stresses is present in the vicinity of the wall, ahead of its face [2,3]. The schematic picture of that distribution is shown in Fig. 1. Unexpected, dangerous tremors may occur near places where intensive, unbalanced stresses exist. The micro-seismic activity in the vicinity of excavations is not necessarily related to the process of opening of new cracks. As seismic

moment tensor analysis shows [4] some events are associated with slips across pre-existing faults or fractures and others are results of coseismic slope closure.

Seismic monitoring in underground mines is the established technique used for investigation of rock mass instability. In the last two decades, microseismic monitoring systems were used in coal mines to gain better understanding of rock mechanics and tremor hazard involved in longwall mining (e.g. [5,6]). Seismic activity takes place ahead of the long wall face as well as behind it; however, the first activity dominates [7]. It is the straightforward effect of the stress increase and rock deformations, for example slip across pre-existing fault or slip associated with fresh fracture. On the other hand, the seismic activity behind the mechanical support is rare and connected with rock mass distressing and roof falling.

Numerous variants of observation setups determine the inspected mine area and the energy band of the events recorded during monitoring. Commonly used, low frequency seismometers may cover the whole mining area. Unfortunately, they record only strong vibrations generated by the highest energy tremors. Such tremors are relatively rare. Most of seismic events have low energy and can only be detected near their sources. In that case, high frequency accelerometers have to be used. Because the number of low energy seismic events is relatively large, it gives an

\* Corresponding author at: AGH University of Science and Technology, al. Mickiewicza 30, 30-059 Kraków, Poland. Tel.: +48 12 6172368.

E-mail address: [lesniak@agh.edu.pl](mailto:lesniak@agh.edu.pl) (A. Leśniak).

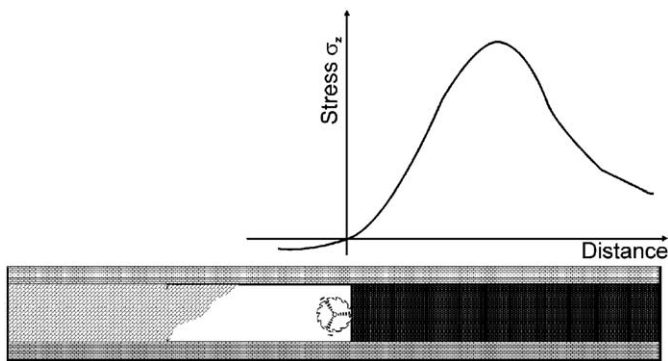


**Fig. 1.** Schematic distribution of vertical stresses in the vicinity of the longwall. The most intensive stresses are concentrated over the coal seam (marked black). The face of the longwall and the coal cutter-loader (marked as a saw disc) are placed at the beginning of coordinate system. On the left the falling rocks form a rubble.

opportunity to perform probabilistic seismic hazard analysis (PSHA) [8]. Such analysis usually follows the process of active source zones locations or clusters identification [9,10].

The main objective of the field work and the analysis presented in this article was to examine the relation between hazard functions evaluated using the events only from one separated cluster and the strong tremors in cluster area. An important topic of the analysis is the correct segmentation of the hypocenters into the clusters assumed to be correlated in time and space. Such a cluster could be regarded as a manifestation of the same dynamic process developing in limited time and space in the mine. Another problem we investigate is the time and space correspondence of the tremors with the parameters of hazard assessment functions evaluated using microseismic events.

The “Zabrze-Bielszowice” coal mine and particularly described coal bed 507 are characterized by high seismic activity and considerable rockburst hazard. The exploitation was conducted on four overlaying panels. The data set analyzed in this article was measured in the bottom panel where the tectonic structure and confining stress distribution were most complicated.

## 2. Method of analysis

Microseismic activity in the vicinity of the longwall panel was recorded using triaxial geophones. For location of the seismic sources, the P wave onsets and P wave polarization were used [11]. Such method is commonly used in the interpretation of microseismic activity in Polish coal and copper mines. It enables source location when the distances between the source and the geophones are so small that the P and S phases are not well separated.

The first approximation of the source location is obtained in ray tracing analysis made for each geophone. The direction of the ray at the particular triaxial geophone is defined by principal eigenvector of the covariance matrix at P wave onset. The source is assumed to be at the point for which the average distance from the rays is minimal. It may be the ray crossing point for some cases. Such first approximation of source location can be used as a starting point for iterative procedure of minimization of the misfit function, which refines the source location. The misfit function expresses the difference between measured and modeled times for the points in the vicinity of the first approximation [12]. The equation that describes the misfit function is non-linear, so besides the global minimum, may consists of many local minima. To find the global minimum, we use the simple Monte Carlo method. The examined points are placed inside the sphere with

the centre in the starting point. The point, which minimizes the misfit function, is the global minimum (i.e. sought hypocenter). The location procedure mentioned above is described and discussed by Mendecki and Sciocatti [13].

Located sources of microseismic events usually form a wide-spread “cloud”. The analysis of the distribution of sources inside the microseismic cloud can provide the information about the system of fractures in the inspected area. Mapping of the fracture distribution and monitoring of its development can help in accessing the current tremors hazard in particular mining area.

There are several methods proposed to identify tectonic structures inside the seismic zone. All these techniques can increase the resolution of the final picture in the sense that the sources directly indicate the location and orientation of the main, active discontinuities in the rock mass. One of the proposed techniques is the “collapsing method” [14]. In that method, the hypocenters are moved towards the centre of mass of the events inside the certain confidence interval. At that interval, they use an error ellipsoid of the original location truncated at a confidence level equal to four standard deviations of the location uncertainty. It corresponds to approximately 99.8% confidence. The located event can reside anywhere within the error ellipsoid so the shifting does not change significantly the RMS misfit to the arrival time data. The method tends to collapse the hypocenters to the simplest structures i.e. points. The original collapsing method has later been developed [15] to collapse the hypocenters not only to the points but also to lines and planes. Such simple structures can represent major tectonic structures connected with the generated acoustic emission. The collapsing method increases the resolution of the seismic cloud by enlarging the density of the sources in some regions (around some points, lines and planes) and decreasing in others. The total number of the events in the cloud remains the same after the collapsing procedure.

The collapsing method is a time consuming algorithm. It works well when the analysis is made off-line. Such analysis can be applied if reconstruction of the static picture of the tectonic structures is more important than the investigation of their dynamic development. Such off-line analysis is sometimes done during hydraulic tests on geothermal or oil fields when we are interested in extent of the geothermal or oil reservoirs. For the case of seismic activity recorded in underground mines, the methods of increasing the resolution of a seismic “cloud” have to allow the continuous increase of “the cloud” and its gradual displacement connected with progressing exploitation. In this case, another method, called clustering, is a better option.

There are many different clustering algorithms. The particular choice depends on the structure of the data and expected benefits from the classification. An overview of the most popular algorithms can be found in [16]. The result of clustering is a set of recognized clusters—each compound of the elements fulfilling the requirements of clustering. To identify clusters of seismic events various sets of parameters can be chosen. For high quality data with clearly distinguished P and S phases, the set of parameters has been proposed by Leśniak and Niitsuma [17]. For each event a simplified envelope of the waveform was used to evaluate three different parameters: ratio of S/P waves, binary sequence of the simplified envelope [17] and the simplified envelope amplitudes. The effectiveness of the clustering based on these parameters was examined for acoustic emission recorded on Clinton Oil Field and Kakkonda Geothermal Field [17].

In our case the data were recorded at small distances from sources, and their waveforms were undisturbed. To evaluate clusters for these data the source locations and origin times were used.

In our study, we compared three algorithms during the interpretation of the data; these include mean minimum distance

clustering (MMD clustering) [18], hierarchical clustering and *K*-means clustering [16]. We used the MMD method to find the most appropriate number of clusters and to identify the clusters. The second and third methods were used for validation of the clustering results. The conclusion that appeared in the paper of Dubes and Jain [19] is that it is better to apply several clustering approaches and check for common clusters instead of searching for a technical measure of validity for an individual clustering.

We describe, essential for this work, the MMD algorithm, because it is not as popular as the two others. It consists of two passes. In the first pass, the mean distance from each hypocenter to its nearest neighbor is estimated. Based on this distance, those outlier hypocenters, located far away from other hypocenters, are removed. In the second pass, the mean distance from the remaining hypocenters to their nearest neighbors is computed. Then into one cluster are grouped events located closer than half new mean distance. The MMD algorithm is non-iterative and can automatically determine the number of clusters. Experimental results also show that the partition generated by the method is more reasonable than that of the *K*-means algorithm in many complicated object distributions [18]. The advantage of the method is small computation complexity and easy classification of the newly localized hypocenters to existing clusters or the creation of new clusters.

As a result of the MMD clustering procedure, we obtained the clusters with a number of individuals that varied from three to more than two hundred. To validate the results of cluster analysis for the established number of clusters, we performed the hierarchical clustering and *K*-means clustering. As final clusters, we accepted the intersections of the particular clusters obtained as a result of the three clustering algorithms. The differences between each clustering method for the “Zabrze-Bielszowice” mine are described and presented in Table 1.

After the clustering procedure, some hypocenters are not classified to any cluster. We can regard them as outliers and they can be removed from the cloud. This will increase the resolution of “the cloud” and divide it into parts. We can analyze each cluster separately from the other, hoping that they are related to regions with increased tremors hazard.

For each recognized cluster, the hazard assessment was realized. The analysis was done using the hazard functions created using onset times of the events  $t_n$  (or intervals between onsets of consecutive events  $u_n = t_{n+1} - t_n$ ) or alternatively events energy  $d_n$  (evaluated as RMS of the event's seismogram). For microseismic activity, the variables  $d_n$  and  $u_n$  can be modeled as a random processes with Weibull probability distribution [20–22]:

$$F(v) = \begin{cases} 1 - \exp(-av^\gamma) & \text{for } v \geq 0 \\ 0 & \text{for } v < 0 \end{cases} \quad (1)$$

where  $a > 0$  and  $\gamma > 0$  are the parameters of the distribution. The variable  $v$  for energy is equal

$$v = \log \frac{d}{d_0} \quad (2)$$

and for time intervals

$$v = \frac{u}{u_0} - 1 \quad (3)$$

Parameters  $d_0$  and  $u_0$  are, respectively, the smallest energy and smallest time interval from the recorded data set. Parameters  $a$  and  $\gamma$  of the Weibull distribution are estimated in a moving time window. We can perform hazard analysis for clusters with sufficient number of events.

For the energy of the events, the hazard function is defined as a coefficient  $\psi$  (expected value  $E(v)$  of random process  $v$  with Weibull distribution, estimated for energy of the events in moving window):

$$\psi(a, \gamma) = \frac{1}{\gamma} a^{-1/\gamma} \Gamma\left(\frac{1}{\gamma}\right) \quad (4)$$

where  $\Gamma$  is a gamma function and  $v$  is given by formula (2). That coefficient is proportional to the size of the events in the particular moment of time.

The hazard function  $\theta$  is based on the intervals between onsets of consecutive events. It is defined as an expected value  $E(v)$  of the process  $v$  with Weibull distribution estimated for intervals between the events in moving window (here  $v$  is given by formula (3)):

$$\theta(a, \gamma) = \frac{1}{\gamma} a^{-1/\gamma} \Gamma\left(\frac{1}{\gamma}\right) \quad (5)$$

It is proportional to the heterogeneity of the microseismic activity process.

As a result, we can obtain the hazard function for any moment of time. Its usefulness can be shown if in some mining area, a causal relationship among low energy, high frequency events and high energy tremor can be found. We show that this is not obvious and seems to be related to the cluster and longwall face relative positions. For the time intervals where function values exceed the mean value, we can expect a higher hazard for a strong tremor.

Concluding, our strategy of microseismic activity interpretation was first to evaluate location of the sources then evaluate the clusters and finally perform hazard assessment for each cluster separately.

### 3. Experiment setup and recorded data

The measurements of the seismic activity were conducted in the “Zabrze-Bielszowice” coal mine located in the Upper Silesia, the region in southern part of Poland. The excavated coal bed 507 was located at average depth of 900 m under the surface. The

**Table 1**  
The result of clustering procedure.

	Cluster's number	x	x	x	x	x	1	2	5	3	6	4
MMD clustering algorithm	Number of events in a cluster	3	4	5	6	7	14	15	24	105	139	219
	Number of clusters	6	10	4	1	1	1	1	1	1	1	1
Hierarchical clustering algorithm	Number of events in a cluster	3	4	5	7	8	13	16	25	109	145	220
	Number of clusters	4	8	1	2	1	1	1	1	1	1	1
<i>K</i> -means clustering algorithm	Number of events in a cluster	3	4	5	6	8	9	14	19	120	135	210
	Number of clusters	6	6	5	1	2	1	1	1	1	1	1

First row—cluster's number (x—small cluster not used in further analysis), second row—number of events in each cluster, and third row—number of clusters with the same number of events.

thickness of coal seam varies from 3.8 to 4.4 m, the angle of dip is  $5^{\circ}$ – $10^{\circ}$  and the general strike is SW. The rocks of proximate roof form thin, alternate layers of clay and arenaceous shale and rare sandstone layers. It is overlaid by 60 m thick sandstone layer of 70 MPa strength. It can result in 60–70 m hanging wall [23]. A system of faults with varying throw (up to 8.0 m) and NW–SE trend was located in the openings close to the longwall.

The longwall exploitation system was applied using a cutting machine. The length of the coal face, where measurements were conducted was about 300 m. During the undisturbed periods of exploitations, the average progress of the wall was 2 m/day. The mechanical support of the shaft was gradually moved with the progressing wall. Behind the support, progressive roof failure has formed a rubble.

The seismic monitoring system used in the experiment consisted of four 28 Hz triaxial geophones located underground. The sampling rate was 8 kHz. The recorded signals were ultimately collected by the main receiving panel and data analysis was done on the computer at the mine office. The digital transmission between concentrators and the computer resulted in dynamic range of the measurement system equal to 90 dB. Detailed description of the measurement system and users experiences can be found in the paper of Isakow and Juzwa [24].

The triaxial sensors were deployed in two shafts perpendicular to the face of the wall. Four vertical boreholes drilled in the roof allowed putting the sensors more than ten meters above the coal seam. A plan view of the mining panel and deployed geophones array are shown in Fig. 2.

Localizing seismic sources with such a small array requires the precise location and orientation of triaxial geophones. The coordinates of sensors were taken from precise surveying of the drilled boreholes. The vertical component of each sensor coincides with the direction of the borehole. To evaluate the directions of planar components of the sensors, it was necessary to make a calibration shooting [24]. As a result of the experiment, the angle correction for each sensor has been established. The corrected orientation of the sensors made the precise ray tracing, indispensable for the source location, possible. The experimental shootings proved that errors of source location for such calibration shots were less than 10 m.

We studied two-month data gathered by the discussed method. After two months, the face of the wall was too close to sensors 2 and 3 and the recorded signals contained too much noise, which made the location difficult. So the two sensors were dismantled and moved to the new locations.

The two-month recording (16.04.2003–23.06.2003) resulted in over 2000 recorded events. After some pause, the monitoring was resumed from 15.07.2003 till 13.08.2003 when it was stopped. The main frequency of the recorded events varied from 50 to 150 Hz while their energies varied from 0.1 J to  $4.7 \times 10^4$  J. Only the good quality events recorded at least by three geophones were located. In the first time interval it was 1145 such events. The time distribution of the located events is presented in Fig. 3a and the locations of events in Fig. 3b. During this period of the experiment, a few observational gaps were caused by power supply breaks.

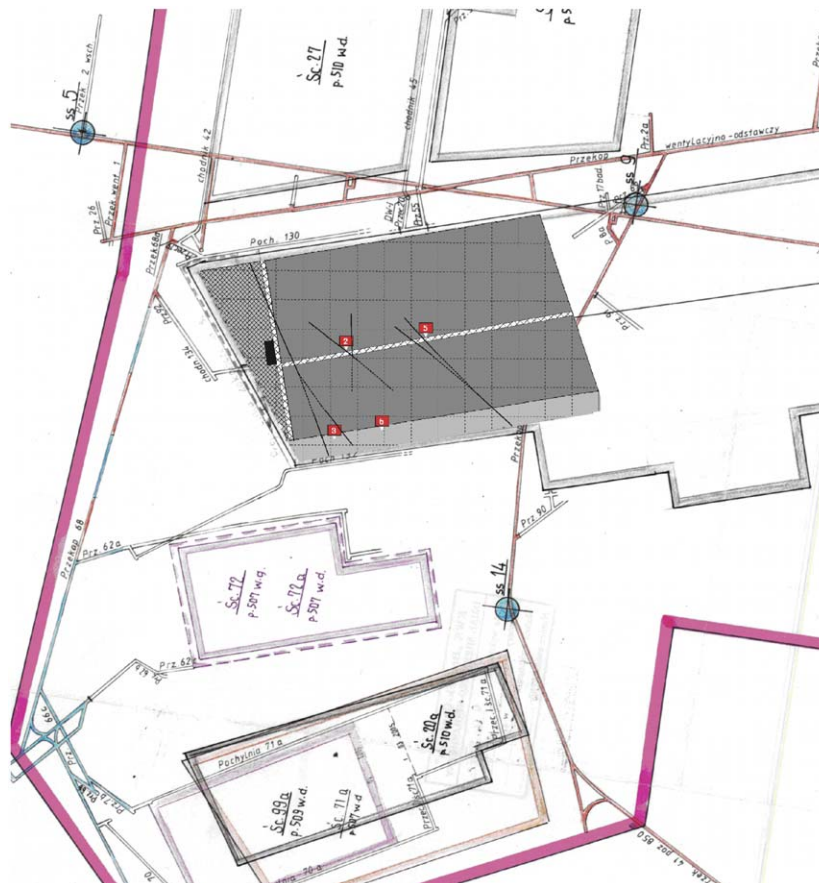


**Fig. 2.** Plan view of the mining panel 306 in coal seam 507, where the measurements were carried out. The geophones deployed in the holes drilled in the roof are numbered as 2, 3, 5 and 6. The layers in the vicinity of the panels are inclined in the SSE direction. The differences in the absolute depth between the pair of geophones (2,5) and pair (3,6) is about 50 m. The lateral extent of the geophones ranges from 100 m (between geophones 3 and 6) to 250 m (between 3 and 5).

The errors of events locations are a result of inexact estimation of the P-wave onset/P-wave polarization in noisy seismograms and inaccurate velocity model. The noise recorded in the seismograms is caused by disturbances generated by mining activity and electrical noise of the monitoring system. Assuming that the average energy of that noise is constant, the S/N ratio depends on events' energy. For small energy events, the location is less accurate comparing to large energy events.

To evaluate the errors of hypocenters location using the method described in the article, we used the Monte Carlo simulation techniques [25]. For established event's energy, we have modeled the source locations assuming normal distribution of the P-wave onset/P-wave polarization errors and normal variation of the velocity model. The error ellipsoid was estimated for every location using 1000 modeled locations. Four error ellipsoids for microearthquakes recorded during the same day are shown in Fig. 3c. Because most of the sources were located higher than the geophones, the ellipsoids were elongated vertically. A detailed examination of their sizes gave the average values of the semi-axes ( $s_x$ ,  $s_y$ ,  $s_z$ ) of the ellipsoids equal to  $s_x = 5$  m,  $s_y = 6.5$  m,  $s_z = 10.5$  m. As our analysis showed, the size of the error of the particular location was mostly influenced by the average distance from the sensors and the energy of the event (noise level).

As it can be seen in Fig. 3b, the distances of the sources from the roof of the excavated panel are less than 70 m. Most of them

are located above the excavation panel, and only 5% of the total amount of the sources is located below the panel level.

#### 4. Clustering and hazard assessment

As a result of the MMD clustering procedure, the population of the events was grouped into 31 clusters with a minimum number of three events in a cluster. The clusters are presented in Table 1. A total number of clustered events are equal to 607 and the number of non-clustered events is equal to 538.

The MMD clustering procedure does not use any limit distance used for cluster classification. It also does not put any limit on the minimum number of events in the cluster. However, the very small clusters (e.g. consisting of less than 10 small energy events) seem to have insignificant importance in creating dangerous tremors. They did not pass the validation procedure, which is also necessary for clustering. To validate the cluster recognized by the MMD method, we performed clustering by two other methods. The results of hierarchical clustering and K-means clustering are presented in Table 1. We have detected at least 90% of events from large clusters by the overlap of different algorithms. In most cases the small clusters created by these three methods consist of different events. We can conclude that swapping events between

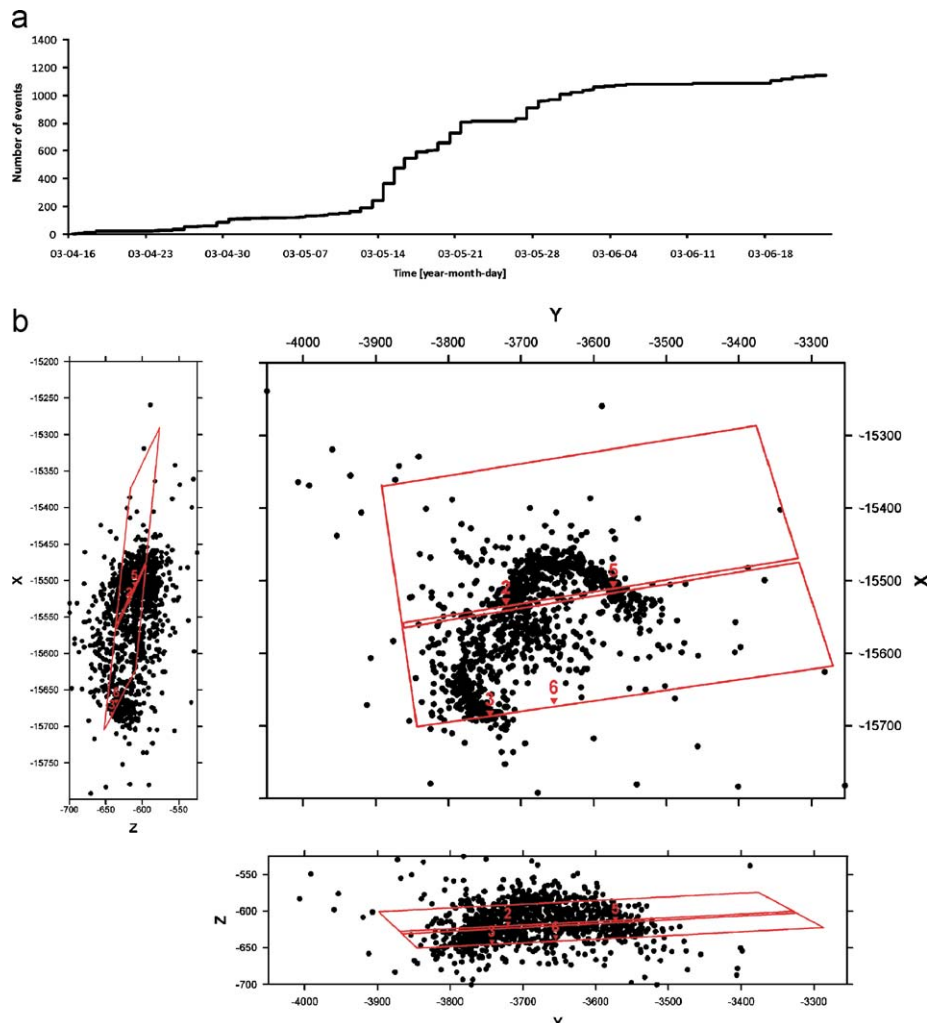


**Fig. 3.** (a) The cumulative number of events located since 16.04.2003–23.06.2003, (b) the locations of events recorded in that period are referenced to local mining coordinate system and (c) example of the error ellipsoids calculated for events recorded during the first day of observations. The vertical semi axes of ellipsoids are more than twice larger than horizontal semi-axes, because of higher uncertainty of the vertical velocity model and distributions of geophones.

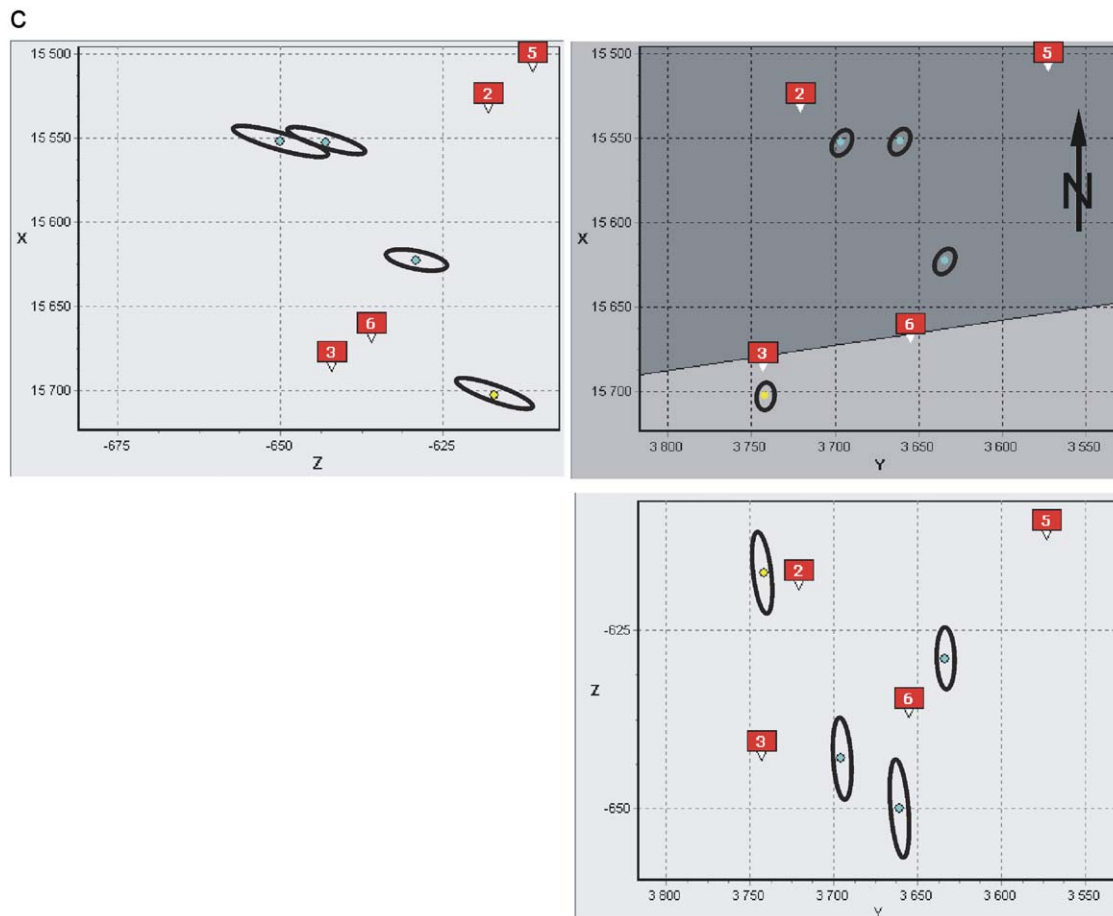


Fig. 3. (Continued)

small clusters appear as a result of erroneous behavior of the clustering algorithms.

In Fig. 4a, the plan and the side views on mining panel and recognized clusters containing more than 10 events are presented. The hypocenters classified to small clusters or unclassified are removed from that figure. We can distinguish six clusters of different sizes, shapes and locations. As it can be seen in the plan (XY) view of Fig. 4, the separation of the clusters in space is very good. Some clusters have an elongated, plane-like shape. Their orientations are similar to the fault system, pre-existed in the roof of the panel. It is shown in Fig. 4a. The other clusters have more irregular shapes, elongated or uniform. Time distribution of the events belonging to the presented clusters is presented in Fig. 5 as the sequences numbered from 1 to 6. The sequence 0 presents unclassified events.

The location of the remaining events (not clustered or clustered to small clusters) is presented in Fig. 4b. Their distribution in space is more uniform and homogeneous than the distribution of the events from the large clusters. The total energy of that group is four times smaller than the total energy of the events constituting the large clusters. Because the number of non-clustered events is, roughly saying, equal to the number of clustered events, the average energy of the first group is four times smaller than that of the second group.

An important question that emerges here is related to the impact of locations errors on clustering results. To inspect this, we relocated the each hypocenter at random distance and direction, within its own error ellipsoid. Then we performed clustering and compared the results with the initial clusters. To compare the related clusters, we checked the number of the events in each

cluster and inspected if the events changed the cluster after relocation. We repeated the calculation 100 times to find how many events changed the recognized clusters. It allowed us to get statistical insight to the problem. In Figs. 6a and b, the clusters before and after relocation, projected on XY plane are presented.

In Table 2, the average number of events that change cluster after relocation is shown for large clusters. Only few events change the clusters after relocation. Similarly, only few events from not clustered group (group 0 from Fig. 5) after relocation were classified to one of the large clusters. It can be the evidence of the small influence of location error on cluster results and analysis. The last statement is true only for large clusters. For small clusters, (e.g. less than six events), the relocation results in more than 50% swap of the events between the clusters. After relocation, seven new clusters were recognized, five of them with three events and two with four events.

As it results from the above discussion, only the cluster with the large number of elements can be used for the evaluation of the hazard functions  $\psi$  and  $\theta$  defined by formulas (4) and (5). These functions were calculated for the period of three weeks, using the energies and time intervals of the events of the largest identified cluster depicted in Fig. 4. Hazard functions are presented in Fig. 7. The parameters of the function were estimated in a three-day moving window. During these time periods, the series of strong tremors was recorded in the overlaying rock mass, more than 70 meters above the roof. They are marked with triangles in the Fig. 6. The distance from the roof is shown in Table 3.

The enlargement of the energy of the seismic events and the heterogeneity of the microseismic activity process reveal an

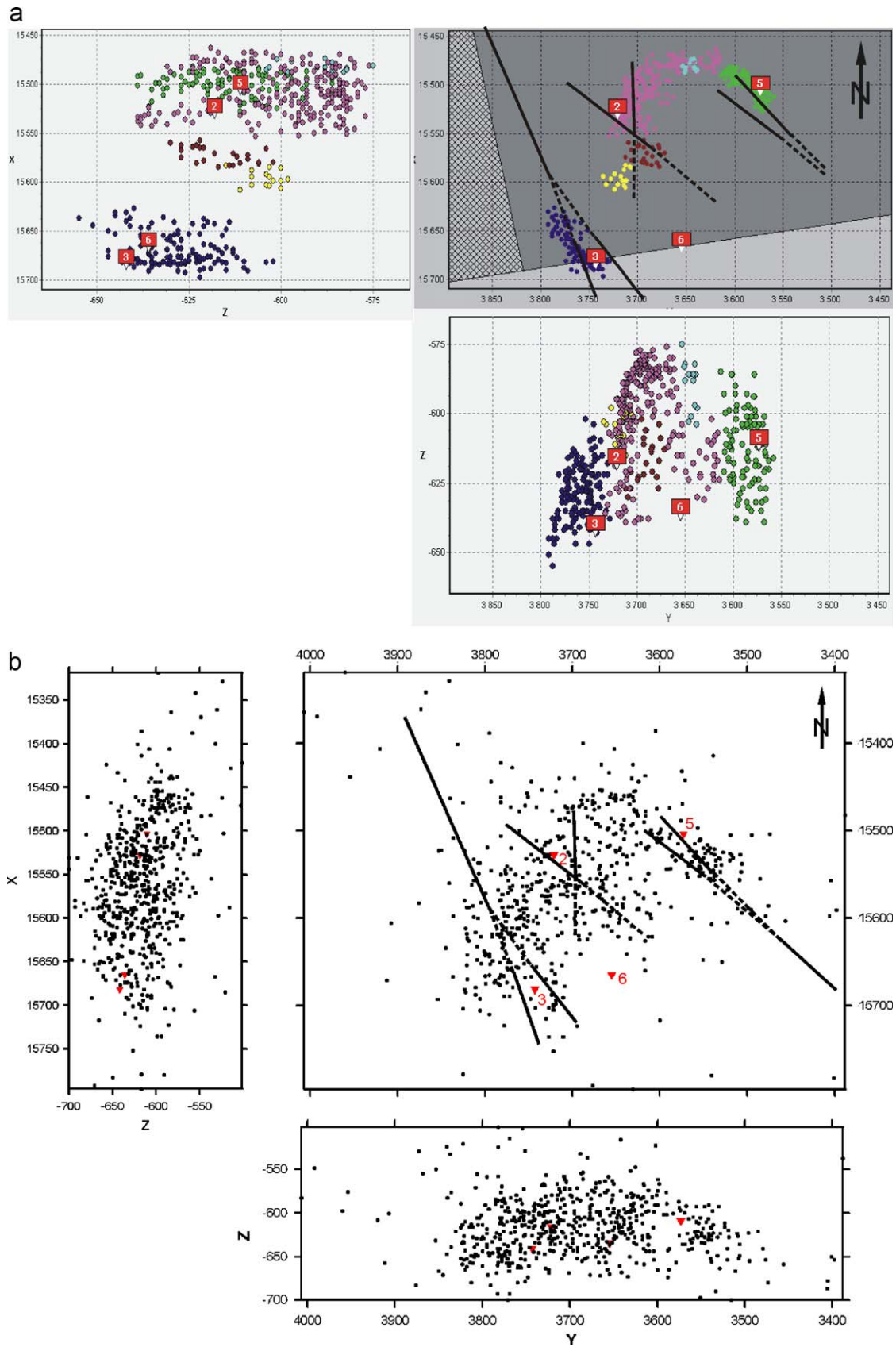


**Fig. 4.** (a) The plane and the side views of the recognized clusters with the minimum number of events in each cluster equal to 10 and (b) the plane and the side views of the non-clustered events.

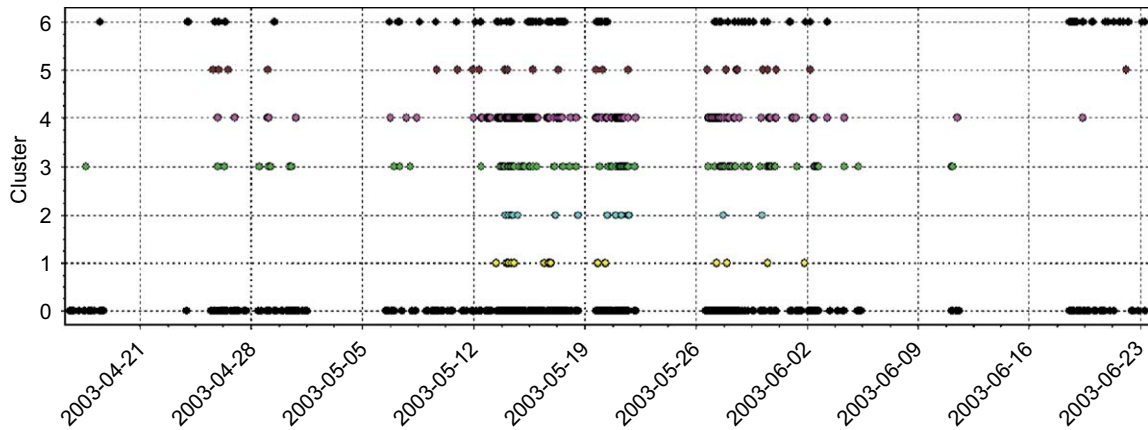


Fig. 5. The time distribution of events in the recognized clusters. The clusters are numbered from 1 to 6.

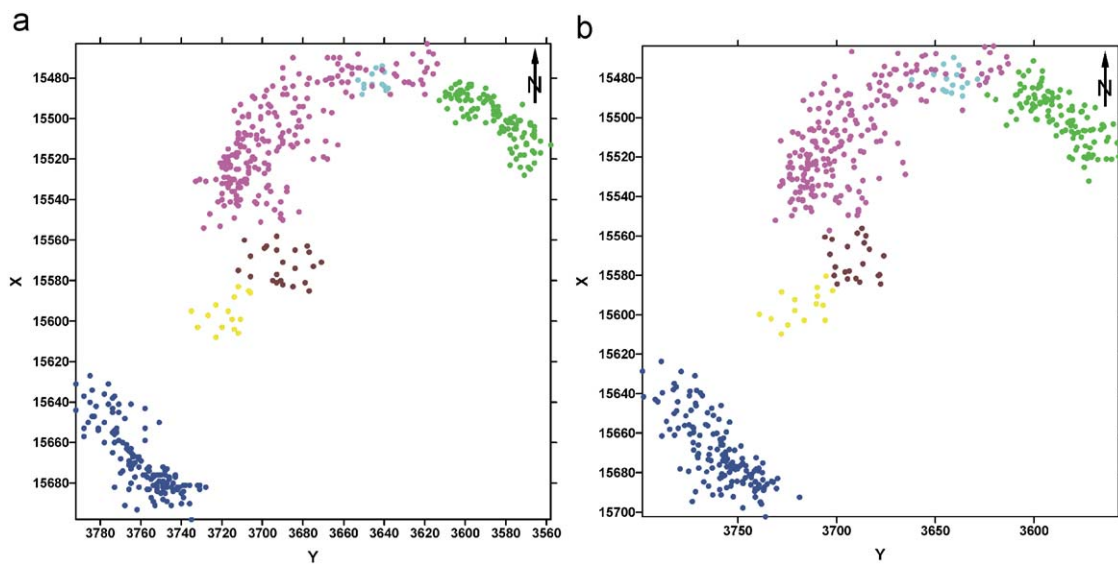


Fig. 6. (a) The projection of the recognized cluster on plane XY before the relocation and (b) the clusters recognized after relocation of each hypocenter within the error ellipsoid. Most of the events do not change the cluster after relocation (see text).

**Table 2**  
Modification of the number of events in large clusters after relocation.

Cluster's number	1	2	5	3	6	4
Number of events in a cluster before relocation	14	15	24	105	139	219
Average number of events that change cluster after relocation (rounded)	0	1	3	3	5	6

increment in the hazard functions  $\psi$  and  $\theta$ . It can be seen that the strongest tremor occurred just after the abrupt drop of the hazard functions.

There is little evidence of strong tremors located inside some cluster (in time and in space). As it can be seen in Table 3, most of the strong tremors are located high above the identified clusters. The locations of the strong tremors in the overlaying beds may be related to the abutments. The abutments create stress concentration zones and may affect the pre-existing faults and fractures above panel 507. The only exception we have found for the analyzed data set is presented in Fig. 8. The cluster created by the events recorded during four days (21.07.2003–24.07.2003) is presented in that figure. The strong tremor (energy  $E = 4.7 \times 10^4$  J) has occurred in the vicinity of the cluster. After it, there was no seismicity in the cluster for more than eight hours.

### 5. Discussion

One of the most important reasons for intensive microseismic activity and tremors in the underground coal mines are the stresses accumulated in the inhomogeneous and cracked rock mass. In the “Zabrze-Bielszowice” coal mine, with exploitation on several mining levels, the stress distribution is particularly complicated. The influence of the overlaying gobs and rubbles may result in stress concentration zones at lower levels. If those zones are located close enough to the current exploration and the roof is cracked or weakened, there is an increase of seismic activity and tremor hazard. In the vicinity of panel 507, there is stress concentration coming from the overlaying panels 506, 502 and 501 shown in Fig. 2. The distribution of high stress zones is heterogeneous and, to a high degree, influenced by pre-existing

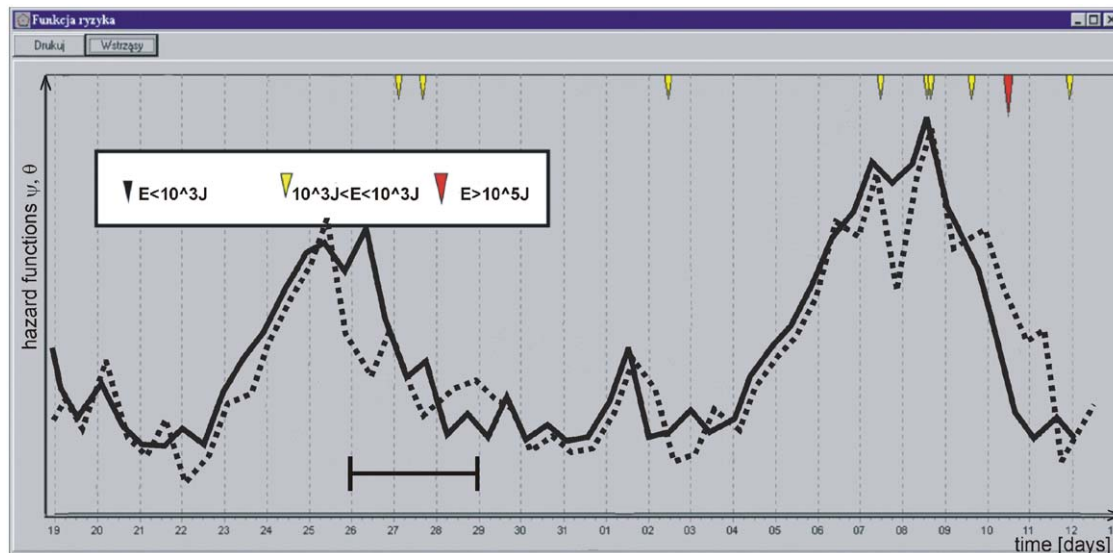


**Fig. 7.** The hazard functions  $\psi$  (solid line) and  $\theta$  (dotted line) defined by formulas (4) and (5) evaluated for the largest (number 4) cluster recognized in “the seismic cloud”. The values of the functions were evaluated with half day step in three-day window indicated in the figure. The triangles show the times when the strong tremors have occurred in the overlaying rock mass.

**Table 3**

Vertical distribution of large tremors.

Distance from roof (m)	Less than 75	75–100	100–125	125–150	More than 150
Number of the strong tremors	1	2	4	4	1

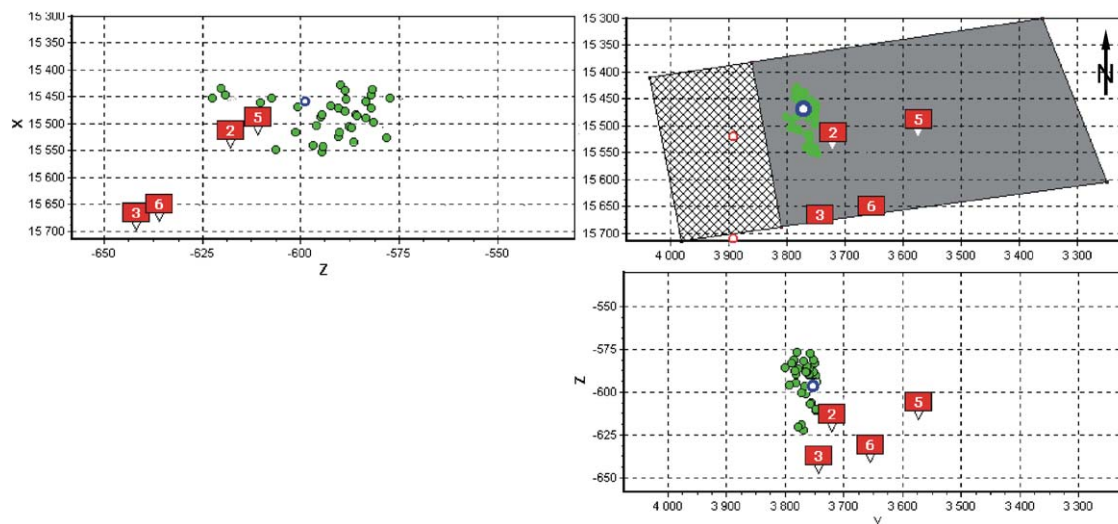


**Fig. 8.** The cluster created by the events recorded during four days (since 21.07.2003–24.07.2003). The strong tremor location is marked as a circle.

faults. We know only the approximate locations of the faults in that area because they can be observed only in two mine galleries. The orientation of the two clusters roughly agrees with the main orientation of those faults. The E–W orientation of the other clusters may indicate the location of the pre-existed or newly created faults not observed in the mine galleries in the vicinity of panel 507.

The total stress distribution is also influenced by stress distribution around the currently excavated panel 507. The vertical distribution of the hypocenters of large cluster events in the vicinity of the panel face is shown in Fig. 9. It can be seen that events located closer to the face of the longwall are also located

deeper. Such distribution generally agrees with the theoretical stress distribution shown in Fig. 1. That relationship is less striking when we compare the theoretical stress distribution with the distribution of all hypocenters (Fig. 3b) or the distribution of non-clustered events (Fig. 4b).

Selected and localized by the MMD procedure, microseismic clusters help to identify the zones with abnormal microseismic activity, where sources were not randomly distributed in space. Those potentially dangerous zones are easily identified because unclassified events have been removed from the analysis. As our analysis shows, few strong tremors originate close to the roof of the exploited panel, in the zone where most of the microseismic

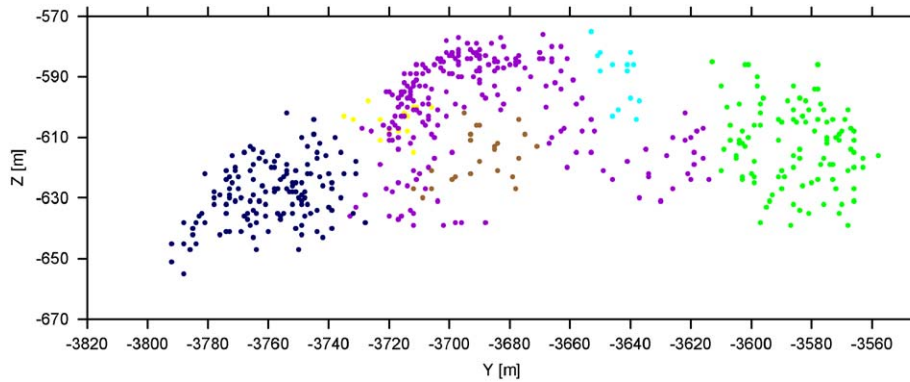


Fig. 9. The vertical distribution of the hypocenters in the vicinity of the panel face shows that events located closer to the face of the longwall are also located deeper.

activity takes place. Most of tremors with epicenters located ahead of the panel face were placed high above the microseismic clusters as it is shown in Table 3. There was almost no microseismic activity detected in the vicinity of the tremors located high above the mining panel. There are two different explanations for this fact. The first is that there was no such emission. The second is that the emission took place but was not registered. It was dumped because of relatively large distance to the sensors. It is risky to give a definitive answer which explanation is correct. The authors assume that the second explanation is more truthful. Two reasons may confirm it. The first one is the observation that the average energy of the microearthquakes located close to the roof of the panel is about three times smaller compared to the average energy located more than 70 m from the roof. The second is the strong heterogeneity of the rocks above panel 507. The stratification of rocks enables easier propagation of waves in the horizontal direction comparing to the vertical one. Those two reasons result in strong energy absorption and lack of evidence of small events.

A definitive answer can be obtained after measurement conducted high above the exploited panels, using sensors in deep boreholes.

An important question is whether the small seismic events are precursors of the rock mass instability that may lead to a strong tremor. If that would be the case, the small events could be used to predict the time and place of a larger tremor. The correlation analysis of small and bigger events made in gold mines in South Africa shows that only in a very few cases, it could be found that microseismic events preceded larger tremors [26]. As the analysis shows, source mechanisms of strong and small seismic events are different in most cases, therefore they could not be correlated and used for prediction. On the other hand, the large events are better correlated in time with the other bigger events in the vicinity [26].

Our analysis made for other coal mines with longwall excavation system shows that there are more examples when such a correlation in time can be observed, if the microearthquakes are localized to clusters. For interpretation made for all events recorded near the panel, the results are negative. The better results can be achieved for hazard functions  $\psi$  and  $\theta$  estimated for clusters confined in space and time. We have experienced numerous examples when the strong tremor or series of consecutive tremors followed the abrupt drop of the hazard functions. We can roughly say that such behavior took place for 75% analyzed tremors. The presented conclusion is unfortunately limited to the longwall excavation system in coal mines.

Because there are almost no microseismic events detected in the gob region, the tremors located there cannot be analyzed in

the way described above. Generally, at the present stage of our experiences we cannot propose any rigorous and quantitative method that based on hazard functions  $\psi$  and  $\theta$  can predict tremor induced by mining activity.

## 6. Conclusions

The analysis presented here can be summarized as follows:

1. Using even a small 3C geophone network (four 3C geophones), we can locate seismic sources with enough accuracy to study the microseismic activity in the rock mass in the vicinity of the longwall panel. Adding new geophones to the array and introducing very precise models for ray tracing can definitely increase accuracy of the hypocenter locations.
2. Clustering of the seismic sources separates the “cloud” into the condensed groups of events and allows indicating the areas where the seismic activity develops most intensively. The projection of the clusters on a horizontal plane coincides with the local faults visible in mine galleries. For most cases (except the one shown above), the depth of the tremor is different from the depth of the corresponding clusters.
3. Hazard functions (estimated using events energy or time intervals) evaluated for particular cluster stay in close inter-relationship with high energy tremors located above the mining panel. In many cases the abrupt drop of the hazard function can be interpreted as a simple indicator of the incoming tremor. Such a factor has only the qualitative meaning.

In conclusion, the study demonstrates the potential of the clustering technique in evaluation of the increment of the seismic hazard over a limited area. Determination of the exact time and place of strong tremors is much more difficult and may prove to be beyond the capabilities of this technology.

## Acknowledgments

We thank anonymous reviewers for valuable comments that helped us to improve this article. Article was written within the framework of a statutory research project of the Faculty of Geology, Geophysics and Environmental Protection, AGH University of Science and Technology, Cracow and EMAG Centre, Katowice, founded by the Polish Ministry of Education and Science.

## References

- [1] Gibowicz S, Lasocki S. Seismicity induced by mining: 10 years later. In: *Advances in geophysics*, vol. 44. New York: Academic Press; 2001. p. 164–81.
- [2] Sałustowicz A. Overview of rock mass mechanics. Katowice, Poland: Wyd. Śląsk; 1965 [in Polish].
- [3] Hudson JA, Harrison JP. *Engineering rock mechanics. An introduction to principles*. Oxford, UK: Elsevier Science Ltd.; 2000.
- [4] McGarr A. Observations concerning diverse mechanisms for mining-induced earthquakes. In: *Proceedings of sixth international symposium on rockburst and seismicity in mines*, Australian Centre for Geomechanics, Western Australia, 2005. p. 107–11.
- [5] Gale WJ, Heasley KA, Iannacchione AT, Swanson PL, Hatherly P, King A. Rock damage characterization from microseismic monitoring. In: *Proceedings of 38th US symposium of rock mechanics*, Washington, DC, 2001. p. 1313–20.
- [6] Luo X, Hatherly P, Gladwin M. Application of seismic monitoring to longwall geomechanics and safety in Australia. In: *Proceedings of 17th international conference on ground control in mining*, Morgantown, WV, USA, 1998. p. 72–8.
- [7] Heasley KA, Ellenberger JL, Jeran PW. Microseismic activity associated with a deep longwall coal mine. In: *Proceedings of SME annual meeting*, Phoenix, Arizona, US, Littleton, Society for Mining, Metallurgy and Exploration, Inc. 2002. p. 1–5.
- [8] Cornell CA. Engineering seismic risk analysis. *Bulletin of Seismological Society of America* 1968;58:1583–606.
- [9] van Aswegen G. Routine seismic hazard assessment in some South African mines. In: *Proceedings of sixth international symposium on rockburst and seismicity in mines*, Australian Centre for Geomechanics, Western Australia, 2005. p. 437–44.
- [10] Lasocki S. Probabilistic analysis of seismic hazard posed by mining induced events. In: *Proceedings of sixth international symposium on rockburst and seismicity in mines*, Australian Centre for Geomechanics, Western Australia, 2005. p. 151–6.
- [11] Flynn EA. Signal analysis using rectilinearity and direction of the particle motion. *Proceedings of IEEE* 1965;53:1874–6.
- [12] Mendecki AJ. Real time quantitative seismology in mines. Keynote lecture. In: *Proceedings of third international symposium on rockburst and seismicity in mines*, Kingstone, Canada, 1993. p. 287–96.
- [13] Mendecki AJ, Sciocatti M. Location of seismic events. In: *Seismic monitoring in mines*. London, UK: Chapman & Hall; 1997. p. 87–107.
- [14] Jones R, Stewart RS. A method for determining significant structures in the cloud of earthquakes. *Journal of Geophysical Research* 1997;102:8245–54.
- [15] Asanuma H, Ishimoto M, Jones RH, Niitsuma H, Phillips WS. A variation of the collapsing method to delineate structures inside a microseismic clouds. *Bulletin of Seismological Society of America* 2001;91:154–60.
- [16] Everitt BS, Landau S, Leese M. *Cluster analysis*. New York, US: Oxford University Press; 2001.
- [17] Leśniak A, Niitsuma H. Clustering similar AE events using the filtered waveform envelope. In: *Proceedings of 13th international acoustic emission symposium*, Nara, Japan, 1996. p. 133–40.
- [18] Peng-Yeng Y, Ling-Hwei C. A new iterative approach for clustering. *Pattern Recognition Letters* 1994;15(2):125–33.
- [19] Dubes R, Jain AK. Validity studies in clustering methodologies. *Pattern Recognition* 1979;11:235–54.
- [20] Rhoades DA, Evison FF. Time-variable factors in earthquake hazard. *Tectonophysics* 1989;167:201–10.
- [21] Lasocki S. Weibull distribution as a model for sequence of seismic events induced by mining. *Acta Geophysica* 1993;41(2):101–12.
- [22] Kagan YY. Statistical aspects of Parkfield earthquake sequence and Parkfield prediction experiment. *Tectonophysics* 1997;270:207–19.
- [23] Dubinski J. Geomechanical and geophysical aspects of the seismicity and rockbursts in N-303 longwall of Bielszowice coal mine. In: *Proceedings of fifth international symposium on rockburst and seismicity in mines*, The South African Institute of Mining and Metallurgy, Johannesburg, RPA, 2001. p. 365–9.
- [24] Isakow Z, Juzwa J. Experiences from using a system for evaluation of dynamic phenomena hazards. In: *Proceedings of sixth international symposium on rockburst and seismicity in mines*, Australian Centre for Geomechanics, Western Australia, 2005. p. 219–26.
- [25] Leśniak A, Pyszczola G. Combined mine tremors source location and error evaluation in the Lubin Copper Mine (Poland). *Tectonophysics* 2008;456:16–27.
- [26] Basson FRP, Ras DJRM. A method to examine the time-space relationship between seismic events. In: *Proceedings of sixth international symposium on rockburst and seismicity in mines*, Australian Centre for Geomechanics, Western Australia, 2005. p. 347–51.